Supporting Information

Strain engineering the electronic and photocatalytic properties of WS_2/blue phosphene van der Waals heterostructure

Jingnan Wang[1], Yuhong Huang[1,*], Fei Ma[2,*], Jianmin Zhang[1], Xiumei Wei[1], Jing Liu[3]

[1] *School of Physics & Information Technology, Shaanxi Normal University, Xi'an 710119, Shaanxi, China*

[2] *State Key Laboratory for Mechanical Behavior of Materials, Xi'an Jiaotong University, Xi'an 710049, Shaanxi, China*

[3] *Department of Basic Sciences, Air Force Engineering University, Xi'an 710051, Shaanxi, China*

*Corresponding authors. Tel.: +86 29 81530750, E-mail: huangyh@snnu.edu.cn (Y.H. Huang),
+86 29 82668610, E-mail: mafei@mail.xjtu.edu.cn (F. Ma).

1. Influences of the calculation parameters during geometric optimization

We have investigated the influences of calculation parameters on the geometric optimization of different stacking structures. The energy cutoff and convergence tolerance of 400eV, 500 eV and 1×10^{-4} eV, 1×10^{-5} eV are successively tested. By these settings, we focus on the variations of bond lengths (W-S, P-P), the layer thickness (WS_2, BlueP) and the minimum distance (d) of four structures corresponding to Model I, II, III and IV. The results are listed in Table S1~4 and the standard errors of the mean ($s_{\bar{x}} = \sqrt{\frac{\sum_{i=1}^{n}(x_i - \bar{x})^2}{n(n-1)}}$) of each physical quantity with different calculation parameters are calculated. It can be seen that the W-S and P-P bond lengths, WS_2 and BlueP layer thickness, as well as the minimum interfacial distance change little with different cutoff energy and convergence tolerance. The values of $s_{\bar{x}}$ are less than 0.008, which indicates the results obtained through the parameters with lower precision are accurate.

Meanwhile, the total energies (E) of each configuration calculated with different parameters are almost maintained, and the standard errors of the mean is only 0.023. Furthermore, the band structures of the most stable heterostructure (Model III) are calculated with different cutoff energy and convergence tolerance, which are depicted in Fig. S1. For comparison, the valence band maximum (VBM), conduction band minimum (CBM) and band gap (Eg) of WS_2/BlueP are calculated and listed in Table S5. The standard errors of the mean of VBM, CBM and Eg are 0.000178, 0.000545 and 0.000723, respectively, indicating the little discrepancy between results obtained via different calculating parameters.

Therefore, WS_2/BlueP is insensitive to the energy cutoff and energy convergence criteria. Considering the computational cost, the cutoff energy and convergence

tolerance of 400eV and 1×10^{-4} eV can be considered reasonable.

Table S1 Geometrical parameters and total energies of WS_2/BlueP heterostructure (Model I).

Model I	cutoff energy (eV), convergence tolerance (eV)				
	400, 1×10^{-4}	400, 1×10^{-5}	500, 1×10^{-4}	500, 1×10^{-5}	$S_{\bar{x}}$ (10^{-3})
W-S length (Å)	2.432, 2.431	2.432, 2.431	2.433	2.433, 2.434	0.364
WS2 thickness (Å)	3.120	3.121	3.123	3.125	1.109
P-P length(Å)	2.249	2.250, 2.249	2.250, 2.249	2.249	0.211
BlueP thickness(Å)	1.264	1.263	1.257	1.259	1.652
d(Å)	3.315	3.337	3.353	3.328	7.983
E(eV)	-294.827	-294.827	-294.904	-294.904	22.228

Table S2 Geometrical parameters and total energies of WS_2/BlueP heterostructure (Model II).

Model II	cutoff energy (eV), convergence tolerance (eV)				
	400, 1×10^{-4}	400, 1×10^{-5}	500, 1×10^{-4}	500, 1×10^{-5}	$S_{\bar{x}}$ (10^{-3})
W-S length (Å)	2.432~2.434	2.431~2.434	2.432~2.434	2.432~2.434	0.274
WS2 thickness (Å)	3.123	3.124	3.123	3.123	0.250
P-P length(Å)	2.250	2.250, 2.249	2.250, 2.249	2.250, 2.249	0.202
BlueP thickness(Å)	1.258	1.258	1.257	1.257	0.289
d(Å)	3.593	3.592	3.593	3.593	0.250
E(eV)	-294.625	-294.624	-294.715	-294.714	25.982

Table S3 Geometrical parameters and total energies of WS_2/BlueP heterostructure (Model III).

Model III	cutoff energy (eV), convergence tolerance (eV)				
	400, 1×10^{-4}	400, 1×10^{-5}	500, 1×10^{-4}	500, 1×10^{-5}	$s_{\bar{x}}$ (10^{-3})
W-S length (Å)	2.432~2.434	2.432~2.434	2.433~2.435	2.432~2.434	0.251
WS2 thickness (Å)	3.124	3.125	3.127	3.124	0.707
P-P length(Å)	2.250, 2.249	2.250, 2.249	2.250, 2.249	2.248~2.250	0.171
BlueP thickness(Å)	1.263	1.262	1.260	1.267	1.472
d(Å)	3.237	3.226	3.266	3.167	20.789
E(eV)	-294.990	-294.990	-295.060	-295.077	22.925

Table S4 Geometrical parameters and total energies of WS_2/BlueP heterostructure (Model IV).

Model IV	cutoff energy (eV), convergence tolerance (eV)				
	400, 1×10^{-4}	400, 1×10^{-5}	500, 1×10^{-4}	500, 1×10^{-5}	$s_{\bar{x}}$ (10^{-3})
W-S length (Å)	2.431~2.434	2.432~2.434	2.432, 2.433	2.432~2.434	0.227
WS2 thickness (Å)	3.123	3.123	3.124	3.127	0.947
P-P length(Å)	2.250, 2.249	2.250, 2.249	2.250, 2.249	2.250, 2.249	0.177
BlueP thickness(Å)	1.259	1.259	1.260	1.260	0.289
d(Å)	3.707	3.706	3.749	3.744	11.594
E(eV)	-294.479	-294.479	-294.568	-294.569	25.837

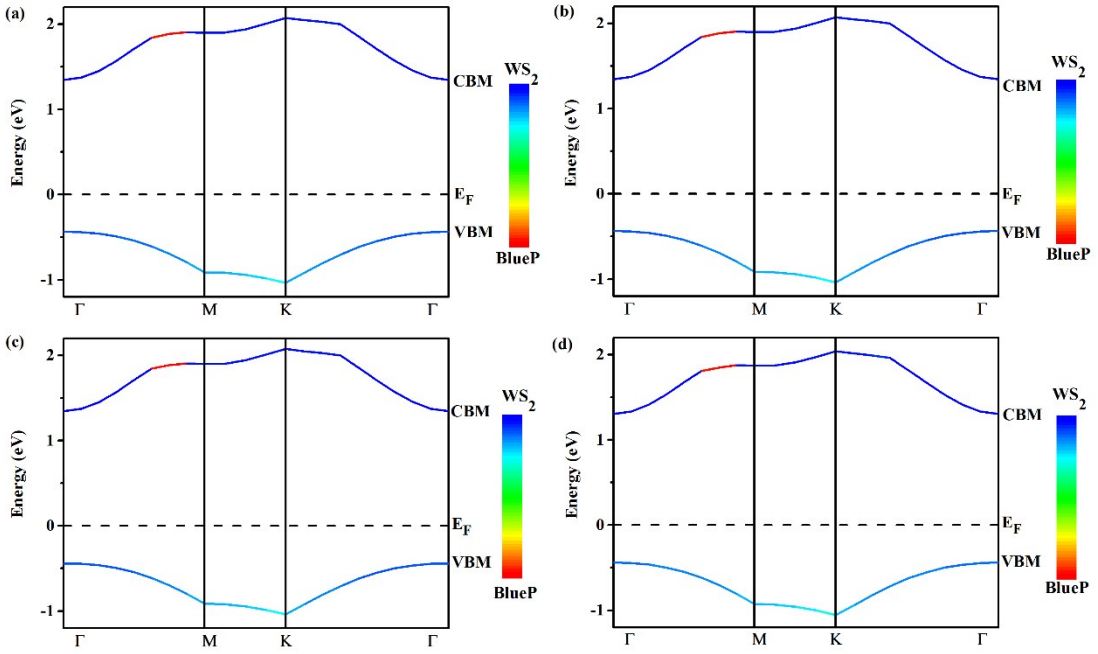

Fig. S1 The band structures of WS_2/BlueP calculating with different energy cutoff and convergence criteria: (a) 400 and 1×10^{-4}, (b) 400 and 1×10^{-5}, (c) 500 and 1×10^{-4}, (d) 500 and 1×10^{-5}. The unit is eV and the Fermi level is set to be zero.

Table S5 The VBM, CBM and band gap of the most stable configuration of WS_2/BlueP.

Model III	cutoff energy (eV), convergence tolerance (eV)				
	400, 1×10^{-4}	400, 1×10^{-5}	500, 1×10^{-4}	500, 1×10^{-5}	$S_{\bar{x}}$ (10^{-3})
VBM (eV)	-0.435	-0.439	-0.435	-0.439	0.178
CBM (eV)	1.344	1.345	1.344	1.306	0.545
Eg (eV)	1.779	1.784	1.779	1.745	0.723

2. Influences of different k-point meshes on the absorption

We have tested the influence of different k-point meshes on the absorption spectrum of the heterostructure. For comparison, the k-point meshes of 2×2×1, 3×3×1, 4×4×1, 6×6×1, 8×8×1 and 15×15×1 are adopted during the computation of optical

properties. The absorption spectra are depicted in Fig. S2. It can be clearly seen that the absorption spectra have converged very well as the k-point reaches 8×8×1. We predict that the absorption spectra will be maintained as the k-point increases to 30×30×1. In view of the computational cost, the 8×8×1 k-point mesh is employed during the investigation of absorption spectra in the paper.

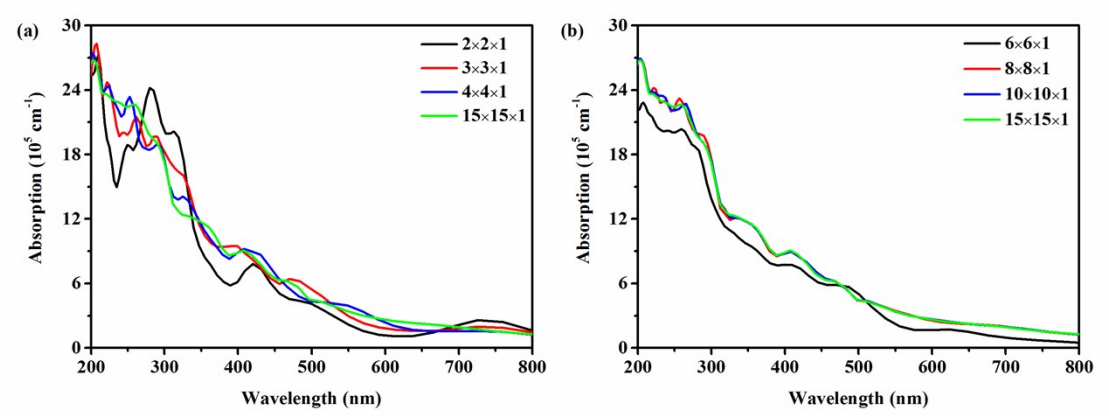

Fig. S2 The absorption spectra of WS_2/BlueP heterostructures calculated via different k-point mesh.

3. Molecular dynamics simulations

We have performed the ab-intio molecular dynamics (AIMD) at room temperature (300K) to evaluate the thermal stability of the WS_2/BlueP heterostructure, since the photocatalytic reactions usually occur at room temperature. The ideal, -4% uniaxial and -6% biaxial strained heterostructures are chosen to perform the AIMD calculations. The time-step is chosen as 1 fs, and 5000 steps are executed. Fig. 3 displays the variation of the free energy and temperature with the simulation time. Obviously, the fluctuation of the free energy are all relatively small during the AIMD simulation, demonstrating the ideal and strained WS_2/BlueP heterostructures are thermally stable at 300 K.

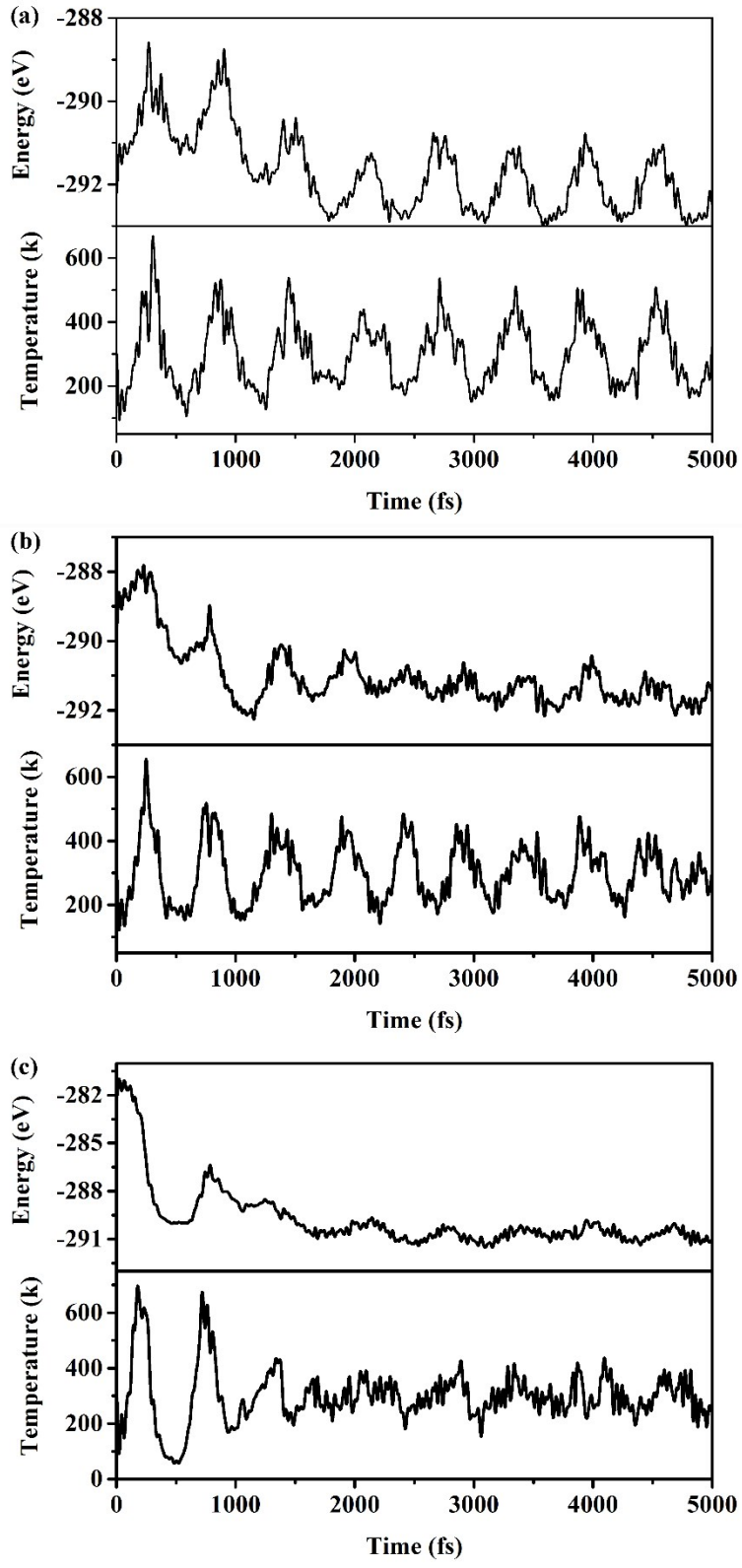

Fig. S3 The variation of free energy and temperature of ideal (a), -4% uniaxial (b) and -6% biaxial (c) strained WS_2/BlueP with simulation time at 300K during a timescale of 5 ps.

4. The effect of uniaxial/biaxial strains on the structural distortion

The relaxed geometrical configurations of uniaxial (-2%, -4%) and biaxial (-2%, -6%, -8%) strained WS_2/BlueP are depicted in Fig. S4. Compared the strained heterostructures with the ideal constructure, it can be seen that there are only slight changes in the optimized geometrical configurations, indicating the stability of the heterostructures.

To investigate the structural distortions, we have calculated the W-S bond length, WS_2 thickness, P-P bond length, BlueP thickness and the minimum interfacial distance (d) of the heterostructure under the strains. Furthermore, the standard errors of the mean ($s_{\bar{x}} = \sqrt{\frac{\sum_{i=1}^{n}(x_i - \bar{x})^2}{n(n-1)}}$) for each strained heterostructure is evaluated, where the $\bar{x}$ is the average value of the ideal heterostructure. The results are shown in Table S6 and S7. The standard errors of the mean of the physical quantities is less than 0.03 and 0.10 for uniaxial and biaxial strained WS_2/BlueP, respectively, indicating that the structural distortion of the system is very small. In summary, the structural deformations of uniaxial and biaxial strained WS_2/BlueP given in our manuscript are acceptable.

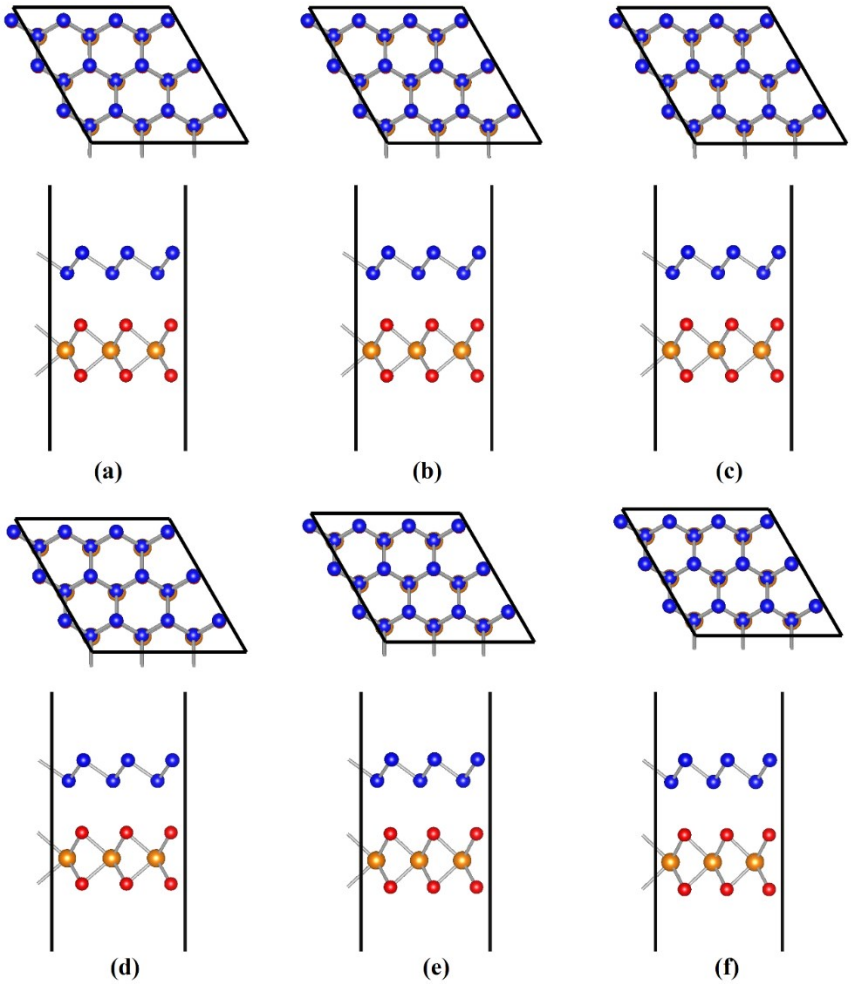

Fig. S4 Optimized geometrical configurations of WS_2/BlueP heterostructures. (a) ideal, (b) -2% uniaxial strain, (c) -4% uniaxial strain, (d) -2% biaxial strain, (e) -6% biaxial strain, (f) -8% biaxial strain.

Table S6 Geometrical parameters of uniaxial strain WS_2/BlueP heterostructure.

physical quantity （Å）	ideal heterostructure	uniaxial strain and standard errors of the mean			
		-2 %	$s_{\bar{x}}$ (10^{-3})	-4 %	$s_{\bar{x}}$ (10^{-3})
W-S length	2.432~ 2.434	2.418~2.426	3.573	2.401~2.438	4.586
WS2 thickness	3.124	3.146	15.556	3.169	31.820
P-P length	2.249~2.250	2.228~2.247	4.478	2.208~2.227	11.001
BlueP thickness	1.263	1.268	3.536	1.275	8.485
d	3.237	3.206	21.920	3.192	31.820

Table S7 Geometrical parameters of biaxial strain WS_2/BlueP heterostructure.

physical quantity	biaxial strain and standard errors of the mean					
（Å）	-2 %	$s_{\bar{x}}$ (10^{-3})	-6 %	$s_{\bar{x}}$ (10^{-3})	-8 %	$s_{\bar{x}}$ (10^{-3})
W-S length	2.418~2.421	6.058	2.397~2.399	14.494	2.387~2.390	19.907
WS2 thickness	3.169	31.820	3.271	103.945	3.324	141.421
P-P length	2.226~2.227	13.282	2.182~2.184	33.253	2.175-2.176	42.725
BlueP thickness	1.275	8.485	1.307	31.113	1.345	57.983
d	3.191	32.527	3.248	7.778	3.225	8.485